

Linear instability of planar shear banded flow

S. M. Fielding*

*Polymer IRC and School of Physics & Astronomy,
University of Leeds, Leeds LS2 9JT, United Kingdom*

(Dated: November 15, 2018)

We study the linear stability of planar shear banded flow with respect to perturbations with wavevector in the plane of the banding interface, within the non local Johnson Segalman model. We find that perturbations grow in time, over a range of wavevectors, rendering the interface linearly unstable. Results for the unstable eigenfunction are used to discuss the nature of the instability. We also comment on the stability of phase separated domains to shear flow in model H.

PACS numbers: 47.50.+d Non-Newtonian fluid flows– 83.60.Wc Flow instabilities – 47.55.Kf Multi-phase and particle laden flows – 61.25.Hq Macromolecular and polymer solutions; polymer melts; swelling

Complex fluids such as wormlike micellar surfactants [1], lamellar onion phases [2], polymer solutions [3] and soft glasses [4] commonly undergo flow instabilities and flow-induced transitions that result in spatially heterogeneous “shear banded” states. This effect is captured by several notable rheological models [5] in which the underlying constitutive curve of shear stress *vs.* shear rate, $T_{xy}(\dot{\gamma})$, is non-monotonic (Fig. 1), allowing the coexistence of bands of differing shear rate at common shear stress, Fig. 2. However, most theoretical studies have considered only one spatial dimension (1D) [6, 7], normal to the interface between the bands (the flow gradient direction, y). The stability of 1D banded profiles in higher dimensions has been implicitly assumed, but is in fact an open question. In this Letter, therefore, we study numerically the linear stability of 1D planar shear banded profiles with respect to perturbations with wavevectors in the interfacial plane (x, z) = (flow, vorticity).

We work within the Johnson Segalman (JS) model [8], modified to include non local diffusive terms [9]. These account for gradients in the order parameters across the banding interface, conferring a surface tension. This “dJS” model is often taken as a paradigm of shear banding systems. Our main result will be that interfacial fluctuations typically grow in time, rendering the 1D banded profile linearly unstable. This potentially opens the way to non trivial interfacial dynamics and could form a starting point for understanding an emerging body of data revealing erratic fluctuations of shear banded flows [10]. This work is a timely counterpart to new techniques for measuring interfacial dynamics [11]. It is also relevant industrially, to processing instability and oil extraction.

The model is defined as follows. The generalised Navier Stokes equation for a viscoelastic material in a Newtonian solvent of viscosity η and density ρ is:

$$\rho(\partial_t + \mathbf{V} \cdot \nabla) \mathbf{V} = \nabla \cdot (\boldsymbol{\Sigma} + \eta \nabla \mathbf{V} - P \mathbf{I}), \quad (1)$$

where $\mathbf{V}(\mathbf{R})$ is the velocity field and $\boldsymbol{\Sigma}(\mathbf{R})$ the viscoelastic part of the stress. For homogeneous planar shear, $\mathbf{V} = y\dot{\gamma}\hat{\mathbf{x}}$, the total shear stress $T_{xy} = \Sigma_{xy}(\dot{\gamma}) + \eta\dot{\gamma}$. The pressure P is determined by incompressibility,

$$\nabla \cdot \mathbf{V} = 0. \quad (2)$$

The viscoelastic stress evolves with dJS dynamics [8, 9]

$$\dot{\boldsymbol{\Sigma}} = 2G\mathbf{D} - \frac{\boldsymbol{\Sigma}}{\tau} + \frac{l^2}{\tau} \nabla^2 \boldsymbol{\Sigma}, \quad (3)$$

with plateau modulus G and relaxation time τ . The non local diffusive term accounts for spatial gradients across the interface between the bands. It arises naturally in models of liquid crystals, and diffusion of strained polymer molecules [12]. The time derivative

$$\dot{\boldsymbol{\Sigma}} = (\partial_t + \mathbf{V} \cdot \nabla) \boldsymbol{\Sigma} - a(\mathbf{D} \cdot \boldsymbol{\Sigma} + \boldsymbol{\Sigma} \cdot \mathbf{D}) - (\boldsymbol{\Sigma} \cdot \boldsymbol{\Omega} - \boldsymbol{\Omega} \cdot \boldsymbol{\Sigma}),$$

in which \mathbf{D} and $\boldsymbol{\Omega}$ are the symmetric and antisymmetric parts of the velocity gradient tensor, $(\nabla \mathbf{V})_{\alpha\beta} \equiv \partial_\alpha v_\beta$. The “slip parameter” a measures the non-affinity of deformation of the viscoelastic component [8]. Slip occurs for $|a| < 1$. The underlying constitutive curve $T_{xy}(\dot{\gamma})$ is then capable of the non-monotonic behaviour of Fig. 1.

Within this model we consider planar shear between infinite, flat parallel plates at $y = 0, L$. We use units in which $G = 1$, $\tau = 1$ and $L = 1$; and boundary conditions at $y = 0, 1$ of $\partial_y \Sigma_{\alpha\beta} = 0 \forall \alpha, \beta$ for the viscoelastic stress, with no slip and no penetration for the velocity.

For an imposed shear rate $\dot{\gamma}$ in the region of decreasing stress, $dT_{xy}/d\dot{\gamma} < 0$, homogeneous flow is unstable [13]. A 1D analysis in the flow gradient dimension then predicts a separation into two bands of differing shear rates $\dot{\gamma}_1, \dot{\gamma}_2$ at common shear stress, T_b , separated by an interface of width $O(l)$. As the applied shear rate $\dot{\gamma}$ is tracked across the banding regime, the relative width-fraction of the bands adjusts to maintain the constraint $\int dy \dot{\gamma}(y) = \dot{\gamma}$, while $\dot{\gamma}_1, \dot{\gamma}_2$ and T_b stay constant, leading to a plateau in the steady state flow curve (Fig. 1).

We verified this 1D scenario by numerically evolving Eqns. 1 to 3, allowing spatial variations only in the flow-gradient direction y . We used a Crank Nicholson algorithm [14] within a finite difference scheme on a uniform mesh of “full” points $y_0, y_1 \dots y_{N_{\text{base}}}$ for $\boldsymbol{\Sigma}$ and staggered “half” points $y_{\frac{1}{2}}, y_{\frac{3}{2}} \dots y_{N_{\text{base}} - \frac{1}{2}}$ for \mathbf{V} . We evolved with time-step Dt for a time t_{max} to steady state, checking for convergence to the limit $N_{\text{base}} \rightarrow \infty, Dt \rightarrow 0, t_{\text{max}} \rightarrow \infty$.

The resulting flow curve is shown in Fig. 1. A typical steady state shear banded profile $\mathbf{V}(y)$, $\boldsymbol{\Sigma}(y)$ is given

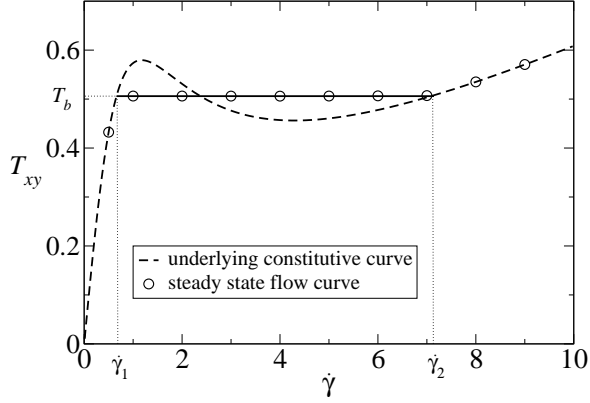


FIG. 1: Underlying constitutive curve; steady state flow curve. $a = 0.3$, $\eta = 0.05$. Banding occurs on the plateau.

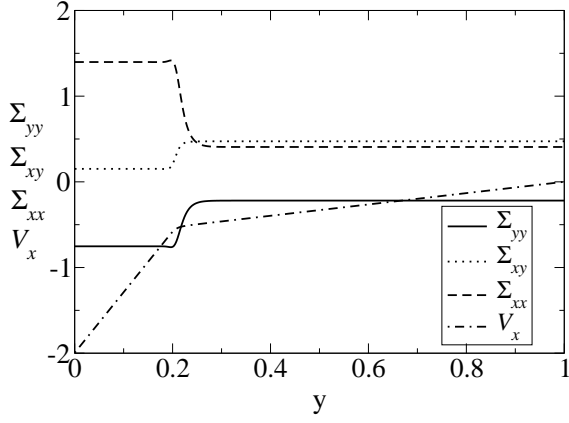


FIG. 2: 1D banded profile, with spatial gradients restricted to the flow gradient direction, y . $\bar{\gamma} = 2.0$, towards the left of the plateau in Fig. 1. $l = 0.01$, $N_{\text{base}} = 800$.

in Fig. 2. The velocity normal to the interface $V_y = 0$ in this 1D profile. The smooth variation of the order parameters across the interface results from the diffusive term in Eqn. 3, which confers an interface width $O(l)$. This is in contrast to local models ($l = 0$) in which the interface is a sharp discontinuity. In fact, local models are pathological in the sense that the banded state is not uniquely selected, but depends on flow history [7, 9].

The linear stability of the sharply banded profiles of local models was studied by previous authors. Renardy [15] found instability with respect to interfacial fluctuations of high wavevector, $q_x \rightarrow \infty$, in the local JS model restricted to the case of a thin high shear band. McLeish [16] studied capillary flow, for general band thickness. He demonstrated a long wavelength ($q_x \rightarrow 0$) instability due to the jump in normal stresses across the interface. This mechanism was also discussed in Ref. [17].

Here we study numerically the *non local* case, in which the 1D banded profile is uniquely selected [7, 9]. The non zero interfacial width, $l \ll L$, now confers a surface tension, which was absent from the local case. We study general band thicknesses and the full (velocity, vorticity)

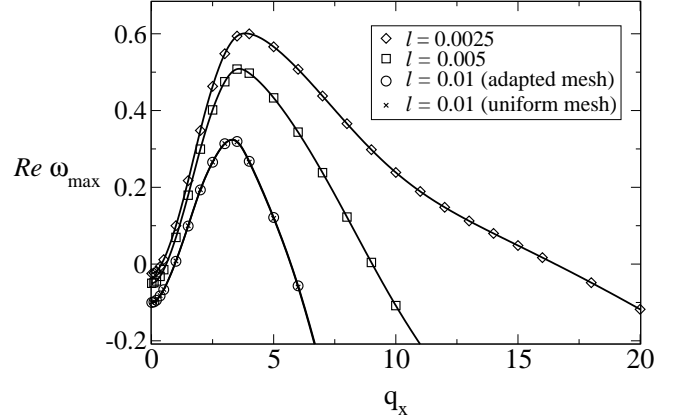


FIG. 3: Real part of the eigenvalue of the most unstable mode. $a = 0.3$, $\eta = 0.05$, $\bar{\gamma} = 2.0$, Reynolds number $\rho/\eta = 0$. The data for $l = 0.01$ correspond to the base profile in Fig. 2. Symbols: data. Solid lines: cubic splines.

plane of perturbation wavevectors (q_x, q_z) .

We linearised the model equations 1 to 3 for small perturbations (lower case) about the (upper case) base profile, $\tilde{\Phi}(x, y, z, t) = \Phi(y) + \phi_{\mathbf{q}}(y) \exp(\omega_{\mathbf{q}} t + i q_x x + i q_z z)$. The vector Φ comprises all components $\Phi = (\Sigma_{\alpha\beta}, V_{\alpha})$, the pressure being eliminated by incompressibility. This linearisation results in an eigenvalue equation with an operator \mathcal{L} , which acts linearly on the perturbation $\phi_{\mathbf{q}}(y)$:

$$\omega_{\mathbf{q}} \phi_{\mathbf{q}}(y) = \mathcal{L}(\Phi(y), \mathbf{q}, \partial_y, \partial_y^2, \dots) \phi_{\mathbf{q}}(y). \quad (4)$$

For numerical study, we discretized this equation on a staggered mesh. The 1D base profile $\Phi(y)$ was read in from the calculation already described. For narrow interfaces, its uniform mesh had too many nodes for use in the eigenvalue problem, so we adapted it to put most attention near the interface. We then used a NAG routine [18] to find the eigenmodes of this discretized problem.

The results, discussed below, were checked as follows: (i) for convergence with respect to mesh structure; (ii) that for a homogeneous base state on the underlying constitutive curve our results match those of Ref. [19]; (iii) that for $a = 0$, $l = 0$ (the local Oldroyd B model), our method gives results consistent with Fig. 3 of Ref. [20]; (iv) that linearisation about a semi-evolved (non-steady) banded state using the *analytically* derived Eqn. 4 gives the same results in the limit $q_x = 0, q_z \rightarrow 0$ as a particular direct *numerical* linearisation performed about the same profile in the code that evolves the 1D base state; (v) for robustness with respect to first evolving the base state on either a uniform or adapted grid, using either a semi-implicit or explicit algorithm; (vi) that two different methods of eliminating the pressure (using the Oseen tensor, and the curl operator) agree.

For any base profile $\Phi(y)$ and wavevector \mathbf{q} , the number of eigenmodes is equal to the number of order parameters summed over all mesh points. In this Letter, we only consider the eigenvalue $\omega_{\text{max}}(\mathbf{q})$ with the largest

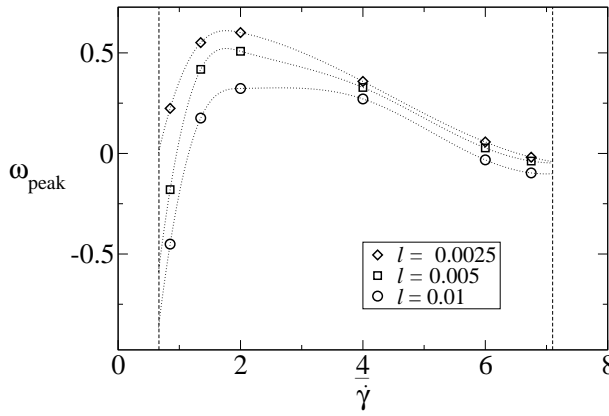


FIG. 4: Peak of the dispersion relation, *i.e.* $\Re\omega_{\max}$ at $d\Re\omega_{\max}/dq_x = 0$. Parameters as for Fig. 3. Limits of the banding regime shown by vertical lines. Symbols: data. Dotted lines: cubic splines, as a guide to the eye.

real part, $\Re\omega_{\max}(\mathbf{q})$. In particular, we ask if this mode is stable, $\Re\omega_{\max} < 0$, or unstable, $\Re\omega_{\max} > 0$. All results given are for a low solvent viscosity $\eta = 0.05 \ll G\tau \equiv 1$, consistent with experiment. We set $a = 0.3$, although our findings are qualitatively robust to variations in a . This leaves the applied shear rate $\bar{\gamma}$ as the tunable parameter.

The dispersion relation $\Re\omega_{\max}(q_x, q_z = 0)$ for fluctuations with wavevector confined to the direction of the unperturbed flow is shown in Fig. 3 for $\bar{\gamma} = 2.0$. At any q_x , $\Re\omega_{\max}$ increases with decreasing l , and for small enough l the dispersion relation is positive over a range of wavevectors, rendering the 1D profile unstable. For small l this applies to shear rates right across the stress plateau of Fig. 1, as shown in Fig. 4. Because the l values accessed here – $l = O(1 - 10\mu\text{m})$ for a 1mm rheometer gap – are even larger than those expected physically, $l = O(100\text{nm})$, our results suggest that, experimentally, the entire stress plateau will be unstable.

In the limit $l \rightarrow 0$, $q_x \rightarrow 0$, the corresponding eigenfunction $\{\partial_y v_x, v_y = 0, \sigma_{\alpha\beta}(y)\}$ tends to the spatial derivative of the base state, $\partial_y \{V_x, V_y = 0, \Sigma_{\alpha\beta}\}$, representing a simple displacement of the interface in the flow-gradient direction, with small corrections in the bulk phases to maintain $\bar{\gamma} = \text{constant}$. As q_x increases from zero, this displacement is modulated by a wave of wavevector $q_x \hat{\mathbf{x}}$ with an eigenvalue $\omega_{\max}(q_x) = \omega_0 + iq_x\omega_1 + q_x^2\omega_2$ with $\omega_2 > 0$, signifying instability. A natural question is whether this instability has the same origin as that described by McLeish for the local model [16]. It is not obvious, *a priori*, that this should be true because, for the base state at least, the limit $l \rightarrow 0$ is singular [7]. Indeed, a detailed analysis (work in progress) is more complicated in this case, and deferred to a longer publication. However, the numerical results of Fig. 5 are qualitatively consistent with the mechanism of McLeish, as follows. A wavelike interfacial displacement with extrema at $q_x x/2\pi = 0.0, 0.5, 1.0$ causes an interfacial tilt near $q_x x/2\pi = 0.25, 0.75$, exposing the normal

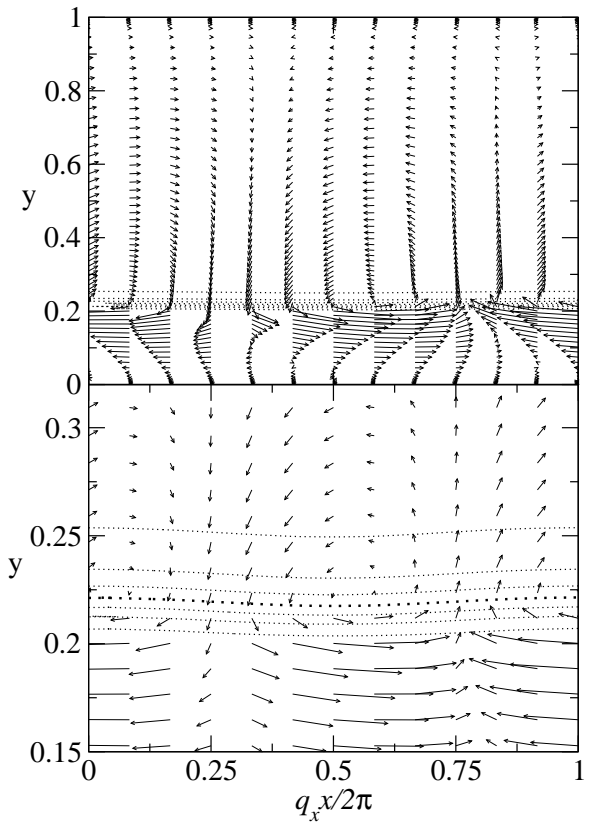


FIG. 5: Perturbation to flow field $s_1 \Re v(y) e^{iq_xx}$ (arrows), and contour lines of perturbed normal stress $\tilde{\Sigma}_{xx}(x, y) = \Sigma_{xx}(y) + s_2 \Re \sigma_{xx}(y) e^{iq_xx}$ (dotted lines), corresponding to the eigenvalue of Fig. 3 with $l = 0.01$, $q_x = 2.0$. Contours downwards: 0.45, 0.60, 0.75, 0.90, 1.05, 1.20, 1.35 (middle value shown thicker). Arbitrary scale factors $s_1 = 1.5$ and $s_2 = 0.3$.

stress jump $\Delta\Sigma_{xx}$ across the interface (recall Fig. 2). This triggers a horizontal perturbation to the flow field $\Im v_x$ in these regions, which recirculates, giving an $O(q_x^2)$ vertical velocity $\Re v_y$ at $q_x x/2\pi = 0.0, 0.5, 1.0$. This enhances the original displacement and so causes instability. Stability is restored for higher q_x (Fig. 3), a feature that is absent in the local case.

The eigenvalue $\Re\omega_{\max}(\mathbf{q})$ over the (q_x, q_z) plane is shown in Fig. 6. Modes with wavevector along the q_x axis are much more prone to instability than those along the q_z axis. Nonetheless, for smaller values of l (not shown), modes along the line $q_x = 0$ can go unstable as well.

We note finally an important bound on the validity of our calculation. The expansion used to obtain Eqn. 4 is valid for perturbations that are small at any point in space. For example, for the stress components we require $\sigma_{\alpha\beta} \ll 1$. Displacement of the interface by a distance Δ gives $\sigma_{\alpha\beta} = \Delta d\Sigma_{\alpha\beta}/dy$, which is $O(\Delta/l)$, because the base profile $\Sigma_{\alpha\beta}$ changes by $O(1)$ over the interfacial width $O(l)$. We are thus restricted to small displacements, $\Delta \ll l$. In future work, we will consider $\Delta \gg l$.

We comment briefly on the stability of a sheared in-

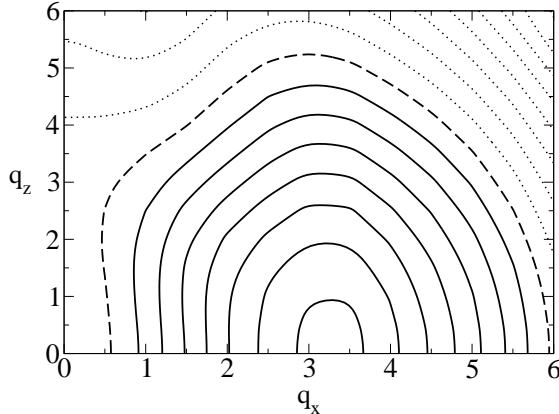


FIG. 6: Real part of the most unstable eigenvalue. $a = 0.3$, $\eta = 0.05$, $\bar{\gamma} = 2.0$, Reynolds number $\rho/\eta = 0.01$ (negligible), $l = 0.01$. Contours are $-0.45, -0.40\dots$ (dotted line), 0.00 (dashed) and $\dots 0.25, 0.30$ (solid).

terface between two phases of a binary fluid in “model H” [21]. Although this was studied in Ref. [22], that work integrated over space to get a simple equation for the position of the interface. Such an approach neglects changes in the interface’s profile, and any fluid flow normal to the interface, so is not guaranteed to agree with ours. Nonetheless, we found the interface to be stable, as in Ref. [22]. This supports the idea that normal stresses (absent in model H) cause the instability described above.

To conclude, we have found 1D planar shear banded flow to be linearly unstable to fluctuations with wavevec-

tor in the plane of the banding interface, within the non local Johnson Segalman model. This applies to shear rates right across the stress plateau, suggesting that the instability is ubiquitous and therefore that the existing theoretical picture of two stable shear bands separated by a steady interface needs further thought. Indeed, our finding is consistent with accumulating evidence for erratic fluctuations [10] and band breakup [23] in several systems. Future work will study the fate of the interface in the non linear regime, beyond the validity of this linear study. One possibility is that the instability is self limiting beyond a critical amplitude set by l (e.g., $l^{1/2}$). This would be consistent with a narrowly localized but still unsteady interface, which might be interpreted as steady in experiments that did not have high spatial resolution. This might even reconcile early data showing apparently steady interfaces with recent work revealing fluctuations.

By contrast, if the instability were found not to be self limiting, and yet ubiquitous in existing banding models (work in progress), one would then need a new theoretical picture of (reasonably) steady shear bands that could still accommodate the required normal stress jump across the interface. Other open questions include the status of the instability in curved Couette geometry; and the relative importance of instabilities at non-zero \mathbf{q} (as studied here) to those found at zero \mathbf{q} in recent models of spatio-temporal rheochaos [24].

The author thanks Paul Callaghan, Mike Cates, Tanniella Liverpool, Tom McLeish, Peter Olmsted and Helen Wilson for useful discussions and feedback; and the EPSRC GR/S29560/01 for funding.

* Electronic address: s.m.fielding@leeds.ac.uk

- [1] M. M. Britton and P. T. Callaghan, Phys. Rev. Lett. **78**, 4930 (1997).
- [2] O. Diat, D. Roux, and F. Nallet, J. Phys. II (France) **3**, 1427 (1993).
- [3] L. Hilliou and D. Vlassopoulos, Ind. Eng. Chem. Res. **41**, 6246 (2002).
- [4] J. S. Raynaud, P. Moucheront, J. C. Baudez, F. Bertrand, J. P. Guilbaud, and P. Coussot, J. Rheol. **46**, 709 (2002).
- [5] M. Doi and S. F. Edwards, *The Theory of Polymer Dynamics* (Clarendon, Oxford, 1989). M. E. Cates, J. Phys. Chem. **94**, 371 (1990). M. Doi, J. Poly. Sci: Poly. Phys. **19**, 229 (1981). P. D. Olmsted and C.-Y. D. Lu, Phys. Rev. **E60**, 4397 (1999).
- [6] N. A. Spenley, M. E. Cates, and T. C. B. McLeish, Phys. Rev. Lett. **71**, 939 (1993). P. D. Olmsted and P. M. Goldbart, Phys. Rev. **A41**, 4578 (1990).
- [7] C.-Y. D. Lu, P. D. Olmsted, and R. C. Ball, Phys. Rev. Lett. **84**, 642 (2000).
- [8] M. Johnson and D. Segalman, J. Non-Newt. Fl. Mech **2**, 255 (1977).
- [9] P. D. Olmsted, O. Radulescu, and C.-Y. D. Lu, J. Rheology **44**, 257 (2000).

- [10] A. S. Wunenburger, A. Colin, J. Leng, A. Arneodo, and D. Roux, Phys. Rev. Lett. **86**, 1374 (2001). R. Bandyopadhyay, G. Basappa, and A. K. Sood, Phys. Rev. Lett. **84**, 2022 (2000). W. M. Holmes, M. R. Lopez-Gonzalez, and P. T. Callaghan, Europhys. Lett. **64**, 274 (2003). Y. T. Hu, P. Boltenhagen, and D. J. Pine, J. Rheol. **42**, 1185 (1998). P. Fischer, E. K. Wheeler, and G. G. Fuller, Rheol. Acta **41**, 35 (2002).
- [11] S. Manneville, J. B. Salmon, and A. Colin, Eur. Phys. J. E **13**, 197 (2004). J. B. Salmon, L. Becu, S. Manneville, and A. Colin, Eur. Phys. J. E **10**, 209 (2003). M. R. López-González, W. M. Holmes, P. T. Callaghan, and P. J. Photinos, Phys. Rev. Lett. **93**, 268302 (2004).
- [12] A. W. El-Kareh and L. G. Leal, J. Non-Newt. Fl. Mech. **33**, 257 (1989). J. L. Goveas and G. H. Fredrickson, Europhys. J. B **2**, 79 (1998).
- [13] J. Yerushalmi, S. Katz, and R. Shinnar, Chemical Engineering Science **25**, 1891 (1970).
- [14] W. H. Press, S. A. Teukolsky, W. T. Vetterling, and B. P. Flannery, *Numerical recipes in C* (Cambridge University Press, Cambridge, 1992).
- [15] Y. Y. Renardy, The. Comp. Fl. Dyn. **7**, 463 (1995).
- [16] T. C. B. McLeish, J. Poly. Sci. B-Poly. Phys. **25**, 2253 (1987).

- [17] E. J. Hinch, O. J. Harris, J. M. Rallison, J. Non-Newton. Fluid Mech. **43**, 311 (1992).
- [18] Numerical Algorithms Group Ltd., Wilkinson House, Jordan Hill Road, Oxford, OX2 8DR, UK.
- [19] S. M. Fielding, P. D. Olmsted, Phys. Rev. E **68**, 036313 (2003).
- [20] H. J. Wilson, M. Renardy, and Y. Renardy, J. Non-Newton. Fluid Mech. **80**, 251 (1999).
- [21] P. C. Hohenberg and B. I. Halperin, Rev. Mod. Phys. **49**, 435 (1977).
- [22] A. J. Bray, A. Cavagna, and R. D. M. Travasso, Phys. Rev. E **6501**, art. no. (2002).
- [23] S Lerouge, PhD Thesis, University of Metz, 2000.
- [24] S. M. Fielding and P. D. Olmsted, Phys. Rev. Lett. **92**, art. no. (2004). Aradian, A and Cates, M E, Pre-print cond-mat/0410509.